Volume 4, Issue 3, 2020 ISSN: 2617-4553
DOI: https://doi.org/10.31058/j.er.2020.43003

Effect of Deposition Time on the Optical, Structural, Electrical and Morphological Properties of Co Doped Zinc Oxide Thin Films by Chemical Bath Method

Egba Augustine Chukwutem[1*], Okpala Uchechukwu Vincent[2], Ottih Ifeyinwa Euphemia[2], Ezenwaka Laz Nnadozie[2]

[1] Physics Advanced Research Centre (PARC), Sheda Science and Technology Complex (SHESTCO), Abuja, Nigeria
[2] Department of Industrial Physics, Chukwuemeka Odumegwu Ojukwu University, Uli, Nigeria

Email Address
egbaaustin@gmail.com (Egba Augustine Chukwutem)
*Correspondence: egbaaustin@gmail.com

Received: 15 October 2020**; Accepted:** 15 November 2020**; Published:** 24 November 2020

Abstract:
In this work, we have demonstrated successfully the deposition of cobalt doped zinc oxide thin films by chemical method. Deposition of nanostructured rod – like films was achieved using zinc acetate and cobalt acetylacetone as cationic precursors. EDTA was used as complexing agent while ammonium solution was employed to stabilize the pH of the reaction bath. The deposited films were characterized to determine their thickness, optical, structural, morphology, composition and electrical properties using stylus profiler (Veeco, Dektak 150), spectrometer (Filmetrics F10 – RT), Bruker AXS (Germany, X – ray diffractometer), scanning electron microscope (Auriga HRSEM) equipped with Energy Dispersive X-ray Spectroscope (EDS) and ECOPIA Hall effect measurement system (HMS - 300) respectively. Results obtained showed that properties of the deposited thin films were affected by deposition time. Absorbance, transmittance and extinction coefficient values varied with deposition time. Energy band gap and film thickness were also affected by deposition time. Film formed after 36 hours was thicker than film deposited after 12 hours. Structural properties of the film confirmed the presence of Zinc oxide with wurtzite structure and grain sizes between the range of 14.90 nm and 21.50 nm. Scanning electron micrographs showed that the film composed of nanorods of slightly different sizes. Composition analysis of the film confirmed the presence of cobalt, zinc and oxygen.

Keywords:
Cobalt Doped Zinc Oxide, CBD, Structural Properties, Optical Properties, Electrical Properties

1. Introduction

Zinc Oxide, which has been a subject of extensive investigations, has been produced commercially for considerable use. Zinc Oxide is classified as II–VI

semiconductor material and it is a very promising material for semiconductor device applications due to its wide range of useful properties [1]. ZnO has a direct wide band gap of 3.44 eV at lower temperatures and 3.37 eV at room temperature, which enables some applications in optoelectronics such as light-emitting diodes, laser diodes and photodetectors [2]. Zinc Oxide has been found to possess diverse nanostructures, such as nanotubes, nanowires, nanorods, nanobelts, nanotetrapods, nanoribbons, nanorings, nanocombs, and so on and these ZnO nanostructures can possibly be grown on cheap and flexible substrates

Many techniques have been used to deposite high quality ZnO thin films. Some of them are electro-deposition technique [3,4,5], pulsed laser deposition [6], RF sputtering [7], chemical solution deposition [8,9,10], the sol – gel method [11,12,13], spray pyrolysis [14,15,16].

This work was aimed at fabricating cobalt doped zinc oxide thin films by chemical bath method. Effect of deposition time on the thickness, optical and electrical properties of the deposited thin films was optimized. X – ray diffraction (XRD) analysis was used to confirm the structure of film formed while scanning electron microscopy (SEM) equipped with energy dispersive x – ray spectroscopy (EDX) was used to determine the surface morphology and elemental composition of the deposited thin film.

2. Experimental Details

Cobalt doped zinc oxide nanostructured thin films were deposited using chemical bath method at varying time. The deposition bath contains zinc acetate and cobalt acetylacetone that served as cationic precursors. Disodium Ethylenediamine Tetraacetate (EDTA) was used as a complex agent to slow down precipitation of metallic ion in the reaction bath while ammonium hydroxide solution was used to stabilize pH of the bath. Prior to deposition, all the glass substrates used in this experiment were first cleansed by immersing them in Piraha solution for three hours, washed with distilled water before usage. Cobalt doped zinc oxide thin film was grown by mixing 10 ml of Zinc Acetate, 2 ml of Cobalt Acetylacetone, 2 ml of EDTA, 0.1 ml of Ammonia Solution and 35.9 ml of distilled water in 100 ml beaker magnetically stirred for 20 minutes, before glass substrate was inserted into the solution. The substrate was made to stand erect by using synthetic foam that also acted as a cover. Five different 100ml beakers were used with bath names ZCT_1 for 12hrs deposition time, ZCT_2, ZCT_3, ZCT_4, and ZCT_5 for different deposition time of 18hrs, 24hrs, 30hrs and 36hrs respectively. Table 1 is a summary of the deposition time optimization for cobalt doped zinc oxide thin films.

Table 1. *Optimization Parameters for Time Variation.*

Bath Name	Dip Time (hrs)	Doping Conc. (%)	ZnAc		CoAcAct		EDTA		NH_4OH		H_2O (ml)
			Mol	Vol (ml)	Mol	Vol (ml)	Mol	Vol (ml)	Mol	Vol (ml)	
ZCT_1	12.00	4.0	0.1	10.0	0.1	2.0	0.1	2.0	0.02	0.1	35.90
ZCT_2	18.00	4.0	0.1	10.0	0.1	2.0	0.1	2.0	0.02	0.1	35.90
ZCT_3	24.00	4.0	0.1	10.0	0.1	2.0	0.1	2.0	0.02	0.1	35.90
ZCT_4	30.00	4.0	0.1	10.0	0.1	2.0	0.1	2.0	0.02	0.1	35.90
ZCT_5	36.00	4.0	0.1	10.0	0.1	2.0	0.1	2.0	0.02	0.1	35.90

3. Results and Discussion

3.1. Measurement of Thickness

The graph of Figure 1 showed that thickness of samples increased as deposition time increased. Sample ZCT_1 had thickness of 0.065µm, ZCT_2 was 0.1µm, ZCT_3 had thickness of 0.14µm, ZCT_4 was 0.51µm and ZCT_5 had a thickness of 0.62µm. We observed that as the time of deposition increased, thickness also increased. This was because more of the ions were deposited on the substrates.

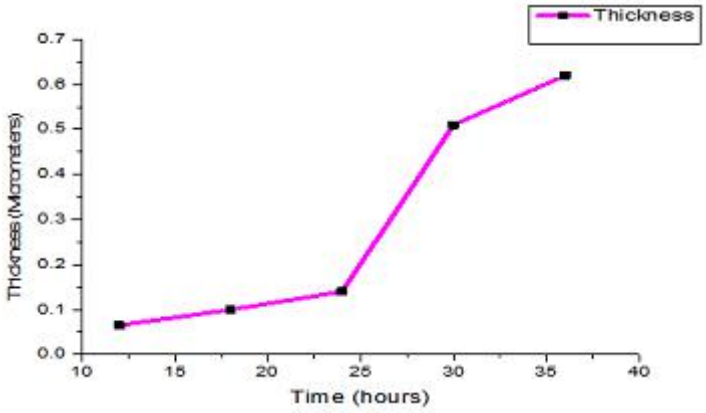

Figure 1. *Graph of Thickness versus Deposition Time for Samples ZCT_1, ZCT_2, ZCT_3, ZCT_4 and ZCT_5.*

3.2. Optical Properties

Optical properties such as absorbance, transmittance, reflectance, refractive index, extinction coefficient, real and imaginary dielectric constants optical conductivity and band gap of the thin films were analyzed within the wavelengths of 250 nm to 400 nm (UV) region, 400 nm to 700 nm (VIS) region.

3.2.1. Absorbance

A plot of Absorbance versus Wavelength for samples ZCT_1, ZCT_2, ZCT_3, ZCT_4 and ZCT_5 is shown in Figure 2.

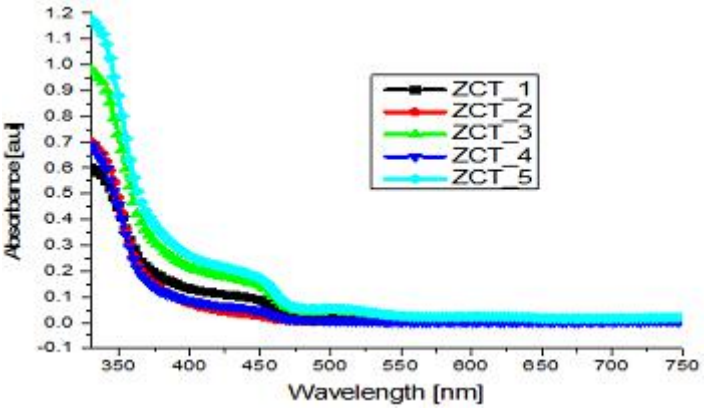

Figure 2. *Plot of Absorbance against Wavelength for ZCT_1, ZCT_2, ZCT_3, ZCT_4 and ZCT_5.*

From the Figure 1, ZCT_1 had maximum absorbance at 340 nm and decreased 15% at 400 nm. ZCT_2 and ZCT_4 have the same level of absorbance in the UV-region with 65% at 340 nm and 10% at 400 nm. ZCT_3 was 95% at 340 nm and decreased to 25% at 400 nm. ZCT_5 had maximum absorbance at 340 nm and decreased to around 25% at 400 nm. In the visible region, difference in absorbance level was noticed within 400 nm to 520 nm. ZCT_1 was 15% at 400 nm, decreased to 6% at 520 nm, ZCT_2 and ZCT_4

had 5% at 400 nm and 4% at 520 nm. ZCT_3 was 20% at 400 nm and decreased to 6% around 520 nm. ZCT_5 was 25% at 400 nm and decreased to 10% at 520 nm. Above 550 nm wavelength, all the samples showed almost zero % absorbance up to 750 nm. Application of such films can be found in UV absorbers for opto-electronic devices. [17].

3.2.2. Transmittance

In the UV-region, ZCT_1 had a transmittance of 25% at 340 nm and then increased to 75% at 400 nm as on Figure 3.

In the UV-region, ZCT_1 had a transmittance of 25% at 340 nm and then increased to 75% at 400 nm as on figure 3. ZCT_2 and ZCT_4 were about 20% at 340 nm and increased to 85% at 400 nm for ZCT_4 and 90% for ZCT_2. ZCT_6 was 10% at 340 nm and increased to 62% at 400 nm. ZCT_5 had 5% transmittance at 340 nm that increased to 55% at 400 nm. At the VIS-region, ZCT_1 had 75% transmittance at 400 nm and increased to 95% at 700 nm. ZCT_2 was 85% at 400 nm but increased to 96% at 700 nm. ZCT_3 had 60% transmittance at 400 nm and 94% at 700 nm. ZCT_4 was 82% at 400 nm increased to 95% at 700 nm. ZCT_5 had 55% transmittance at 400 nm rose to 94% at 700 nm. Such films can be utilized in poultry applications and other optoelectronics devices.

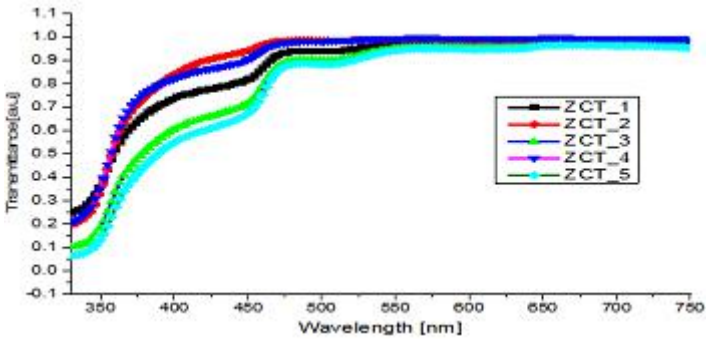

Figure 3. *Plot of Transmittance against Wavelength for Samples ZCT_1, ZCT_2, ZCT_3, ZCT_4 and ZCT_5.*

3.2.3. Reflectance (R)

In Figure 4 there were a general decrease in reflectance in the UV region from 370 nm to 400 nm.

In Figure 4, there was general decrease in reflectance in the UV region from 370 nm to 400 nm. ZCT_1 had reflectance of 1.75 at 370 nm which decreased to 0.08 at 400 nm. ZCT_2 had reflectance of 0.16 and 0.07 at 400 nm. ZCT_2 was 0.2 at 370 nm wavelength and 0.17 at 400 nm. ZCT_4 had value of 0.16 at 370 nm reduced to 0.1 at 400 nm. ZCT_5 had reflectance of 0.2 at 370 nm and 0.18 at 400 nm. In the visible region the decrease continued with ZCT_1 0.07 at 400 nm down to 0.02 at 700 nm. ZCT_2 had value of 0.06 at 370 nm and decreased to 0.02 at 700 nm. ZCT_3 was 0.1 at 400 nm and 0.025 at 700 nm. ZCT_4 was 0.1 at 400 nm and decreased to 0.02 at 700 nm. ZCT_5 had reflectance of 0.18 at 400 nm and 0.025 at 700 nm. This make them suitable for application in poultry houses as antireflective coatings material.

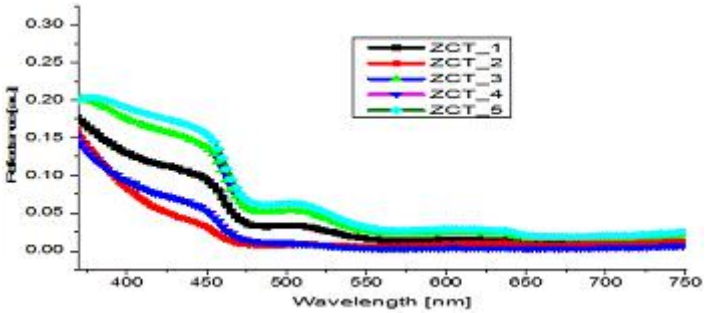

Figure 4. *Plot of Reflectance against Wavelength (nm) for ZCT_1, ZCT_2, ZCT_3, ZCT_4 and ZCT_5 thin films.*

3.2.4. Refractive Index

The refractive index of samples ZCT_1, ZCT_2, ZCT_3, ZCT_4 and ZCT5 were plotted against wavelength (nm) as shown in Figure 5.

In the high UV and low visible region (350-500) nm, all exhibited decreased in refractive index as wavelength increased. ZCT_1decreased from 2.6 at 350 nm to 1.5 at 500 nm. ZCT_2 decreased from 2.6 at 350 nm to 1.25 at 400 nm. ZCT_3 was 2.6 at 350 nm 1.6 at 500 nm. ZCT_4 decreased from 2.6 at 350 nm to 1.25 at 500 nm. ZCT_5 was 2.6 at 350 nm but decreased to 1.6 at 500 nm. From 500 nm to 700 nm, ZCT_3 and ZCT_5 decreased further from 1.6 to 1.4, ZCT_1 also decreased from 1.5 to 1.3. ZCT_4 remained at 1.25 while ZCT_5 increased slightly.

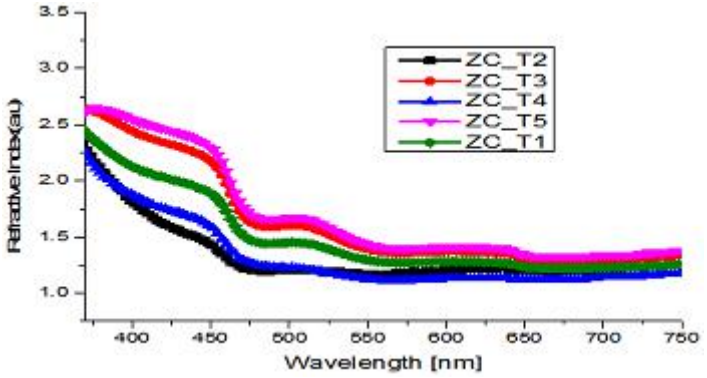

Figure 5. *Plot of Refractive Index against Wavelength (nm) for Samples ZCT_1, ZCT_2, ZCT_3, ZCT_4 and ZCT_5.*

3.2.5. Extinction Coefficient

From Figure 6, all the samples showed peak value at 340nm of wavelength. ZCT_5 had the highest peak of 0.38 followed by ZCT_4 of 0.35, ZCT_3 was 0.18, ZCT_2 was also 0.18 and ZCT_1 was 0.25.

In the UV-region, ZCT_1 had value of 0.25 at 340 nm and decreased to 0.07 at 400 nm. ZCT_2 had value of 0.18 at 340 nm and decreased to 0.04 at 400 nm. ZCT_3 decreased from 0.18 at 340 nm to 0.05 at 400nm. ZCT_4 was to 0.35 at 340 nm and decreased to 0.05 at 400 nm. ZCT_5 was 0.38 at 340 nm and then decreased to 0.1 at 400 nm. At the visible region, ZCT_1 decreased from 0.06 at 400 nm to almost 0.01 at 700 nm. ZCT_2 had the same value at 0.01 from 400 nm to 700 nm. ZCT_3 decreased from 0.05 at 400 nm to 0.01 at 700 nm. ZCT_4 was 0.05 at 400 nm which reduced to about 0.01 at 700 nm.ZCT_5 was 0.1 at 400nm but decreased to 0.1 at 700 nm.

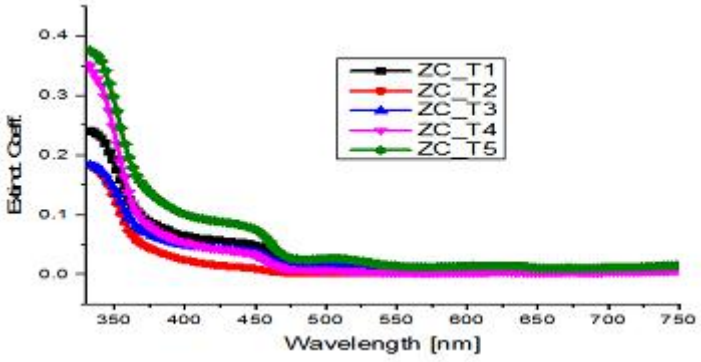

Figure 6. *Plot of Extinction Coefficient versus Wavelength for Samples ZCT_1, ZCT_2, ZCT_3, ZCT_4 and ZCT_5.*

3.2.6. Real and Imaginary Dielectric Constants

The graph of real dielectric constant of samples ZCT_1, ZCT_2, ZCT_3, ZCT_4 and ZCT5 is shown in Figure 7(a) while the imaginary counterpart is shown in figure 7(b).Within the UV-region in figure 7(a), all the samples exhibited decrease in value. ZCT_1decreased from 7.0 at 350 nm to 4.5 at 400 nm, ZCT_2 was 7.0 at 350 nm and 3.5 at 400 nm, ZCT_3 was 7.0 at 350 nm and 5.0 at 400 nm. ZCT_4 had value of 7.0 at 350 nm then decreased to 3.5 at 400 nm. ZCT_5 decreased from 7.0 at 350 nm to 6.5 at 400 nm. In the (VIS) region, it decreased further with ZCT_1 having a value of 4.5 at 400 nm and 2.0 at 700 nm. ZCT_2 was 3.5 at 400 nm and 2.0 at 700 nm. ZCT_3 decreased from 6.3 at 400 nm and decreased further to 2.2 at 700 nm. ZCT_4 was 3.5 at 400 nm and 1.8 at 700 nm. ZCT_5 decreased from 6.5 at 400 nm to 2.2 at 700 nm.

From Figure 7(b), in the high (UV) and low (Vis) region (from 350 nm to 460 nm), ZCT_1 decreased from 1.0 at 350 nm to 0.1 at 460 nm, ZCT_2 was 0.65 at 350 nm and 0.0 at 460 nm. ZCT_3 was 0.55 at 350 nm and 0.0 at 460 nm. ZCT_4 decreased from 1.25 at 350 nm to 0.0 at 460 nm. ZCT_5 exhibited an irregular behaviour, it increased from 0.25 at 350 nm to 0.27 at 370 nm and then decreased to 0.0 at 46 nm. All the samples remained at 0.0 from 450 nm to 700 nm in the visible region.

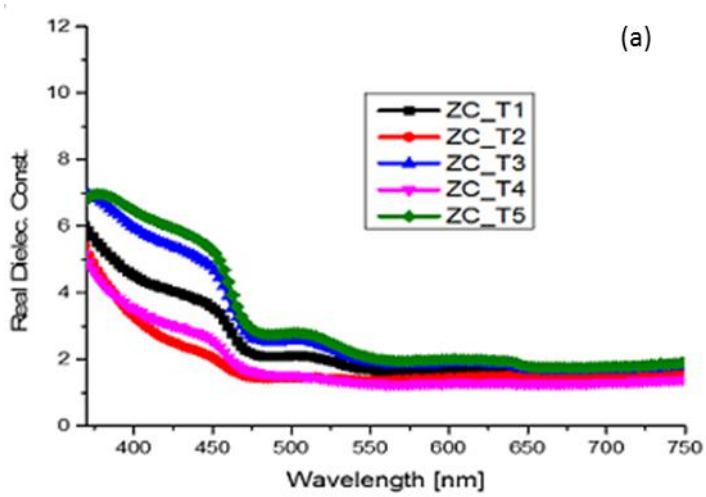

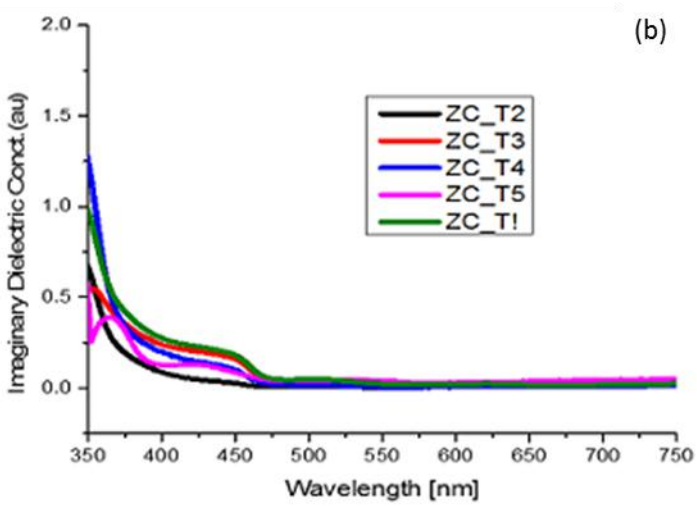

Figure 7. *(a) Plot of Real Dielectric Constant against Wavelength (nm), (b) Plot of Imaginary Dielectric Constant against Wavelength for Samples ZCT_1, ZCT_2, ZCT_3, ZCT_4 and ZCT_5.*

3.2.7. Optical Conductivity (σ_0)

A plot of optical conductivity against wavelength for samples ZCT_1, ZCT_2, ZCT_3, ZCT_4 and ZCT_5 is shown in Figure 8. In all the samples on Figure 8, optical conductivity was observed from 350 nm to 450 nm wavelength. ZCT_1 had a value of 1.5 x 10^{13} S^{-1}at 350 nm and decreased to 0.1 x 10^{12}(1.0 x 10^{11})S^{-1}at 500 nm. ZCT_2 decreased from 1.0 x 10^{13} S^{-1}at 350 nm to 1.0 x 10^{11} S^{-1}at 500 nm. ZCT_3 was 8.0 x 10^{12} S^{-1} at 350 nm and 1.0 x 10^{11} S^{-1} at 500 nm. ZCT_4 is 2.0 x 10^{11} S^{-1} at 350 nm and 1.0 x 10^{11} S^{-1} at 500 nm. ZCT_5 decreased from 2.0 x 10^{12} S^{-1} at 350 nm to 1.0 x 10^{11} S^{-1} at 500 nm. From 500 nm to 700 nm, all the samples showed little or no optical conductivity. Due to this characteristic, the deposited film can be used to trap UV-light for opto-electronic applications. Optical conductivity decreased generally with increase in deposition time.

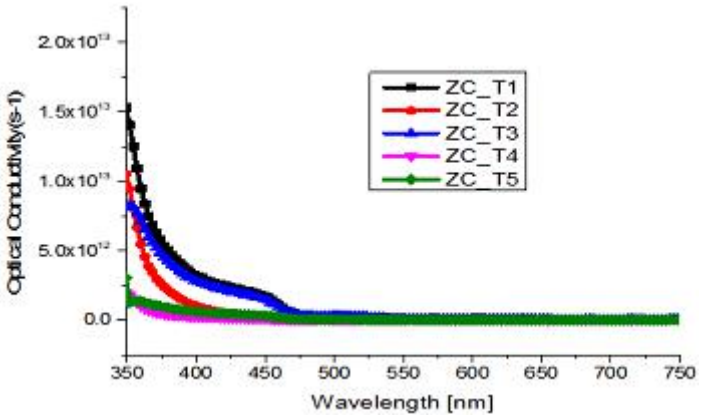

Figure 8. *Graph of Optical Conductivity against Wavelength (nm).*

3.2.8. Band Gap Energy

By extrapolating the straight portion of the graph to the axis of photon energy (*hv)* where $(\alpha hv)^2$ is equal to zero, as shown in Figure 9 (a) and (b) above, we obtain the direct band gap of the films. The band gap of the deposited sample increased gradually as deposition time increased and then fell again, increasing from 3.38 eV to 3.41 eV and then decreased to 3.39 eV, ZCT_1 had a band gap of 3.38 eV, ZCT_2 was

3.39 eV, ZCT_3 was 3.41 eV, ZCT_4 was 3.40 eV and ZCT_5 had a value of 3.39 eV. The deposited films have large band gaps. These deposited films can be utilized in solar cells as absorber layer for energy harnessing [18]. They are also wide band gap materials and can be used in high temperature and high power devices, [19].

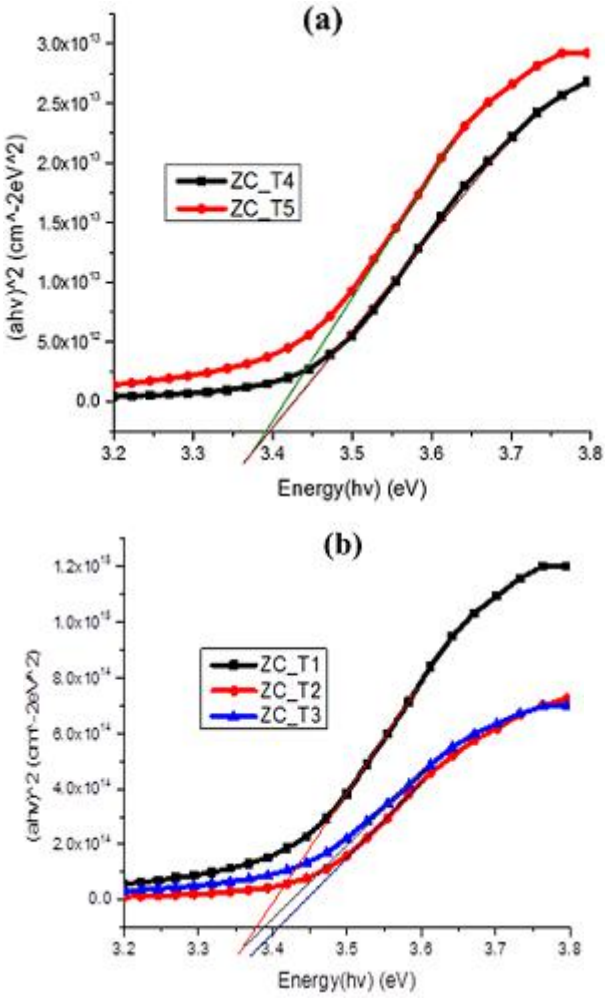

Figure 9. *(a): plot of $(\alpha hv)^2$ against (hv) for samples ZCT_1, ZCT_2 and ZCT_3 (b): Plot of $(\alpha hv)^2$ Vs (hv) for samples ZCT_4 and ZCT_5.*

3.3. Structural Analysis

In Figure 10, the sample indicated a polycrystalline hexagonal wurtzite structure typical of Zinc Oxide (ZnO), (JCPDS card .79 - 0205).

Reflections at 2theta angles of 31.83o, 34.44o, 36.33o, 44.760, 56.86o and 66.340 were conspicuously visible, this corresponds to orientation planes of {100}, (002), (101), {102}, {110} and {200} respectively. The preferred plane of orientation being that of {100}, followed by {110}, {002}, and {101} as shown in Figure 10. Various parameters deduced from the XRD – pattern of the characterized sample were shown in table 2. The lattice constants, a = b and c have been calculated to be, 3.244 Á and 5.347Á respectively. These values are in good agreement with those of [20, 21]. Microstrain, the mismatch between the substrate and the film was also calculated to be 0.644.

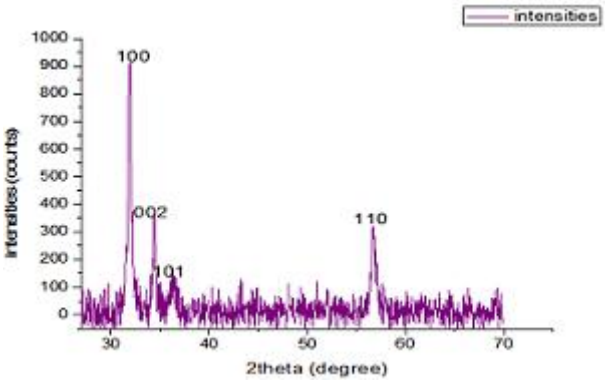

Figure 10. *Plot of intensities versus 2 theta for sample ZCT_4.*

Table 2. *Parameters deduced from the XRD – pattern of sample ZCT_4.*

2theta		(hkl)	FWHM (β) (°)	Average Grain Size (D) (nm).	Dislocation density (ρ) x 10^{15}	Interplaner spacing (A^0)
Standard	Recorded					
31.770	31.830	100	0.70	21.50	2.16	3.244
34.422	34.440	002	0.74	20.05	2.49	1.622
36.253	36.330	101	1.02	14.92	4.49	2.294
56.603	56.860	110	0.90	17.71	3.19	2.294

3.4. Microstructural/Compositional Analysis

Figure 11(a) is the micrograph of sample ZCT_4 using SEM measurements. The surface image illustrated a film that was not closely packed but homogenous in clustered form and was rod-like (nanorods).

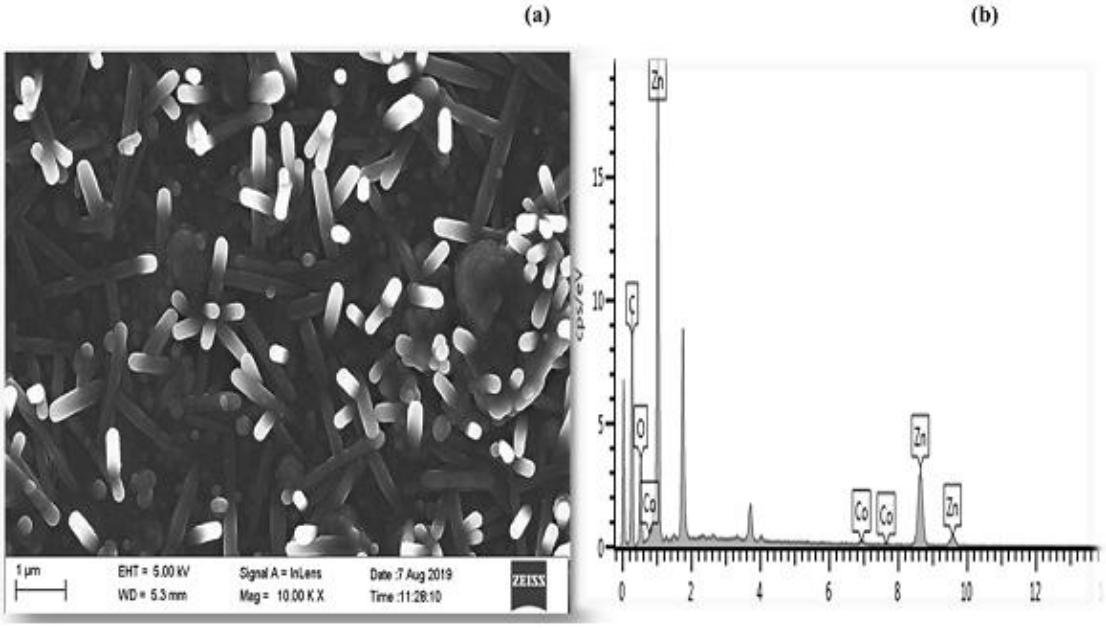

Figure 11. *(a) SEM image of sample ZCT_4 . (b) Energy Dispersive X-ray Spectroscopic Spectra of ZCT.*

The homogeneity was an indication that the dopant, cobalt (Co) substituted zinc site in ZnO compound very well and do not contain any other dopant dominating phase. This is due to the fact zinc ions and cobalt ions have close atomic radius (Zn^{+2}=60A^o and Co^{+2}=58 A^0) [22,23]. The Energy dispersive X-ray spectroscopy (EDS)/EDX) result of the sample shown in figure 11(b), above indicated the presence of elements

Zinc (Zn) with 48.64 % atomic weight, Oxygen (O) with 12.18 % atomic weight and Cobalt (Co) with 3.17 % atomic weight as the main elements of the film ZCT_4 which was expected. The presence of Carbon peak (C) with 36.01 % in the spectra was suggested to emanate from the precursor compounds.

3.5. Electrical Properties

Table 3 is the effect of deposition time on electrical properties of samples ZCT_1, ZCT_2, ZCT_3, ZCT_4 as measured by Hall Effect measurement system. Samples ZCT_1, ZCT_2, ZCT_3, and ZCT_4 measured, showed n-type semiconductor/conductivity as indicated by their negative hall coefficient (R_H), [24]. Their n-type conductivity was also affirmed by their negative bulk concentration (N_b) values. Resistivity increased generally as deposition time increased while conductivity exhibited no trend. Hall coefficient also increased as deposition time increased.

Table 3. *Electrical properties of ZCT_1, ZCT_2, ZCT_3 and ZCT_4.*

Sample Name	Time (hrs)	Nb (cm^{-3}) $X10^{12}$	$\mu\left(\frac{cm^2}{Vs}\right) \times 10^1$	Rs (Ω) X 10^6	$\rho(\Omega - cm) \times 10^3$	$\sigma\left(\frac{1}{\Omega - cm}\right)$x 10^{-5}	$R_H\left(\frac{cm^3}{c}\right)$ X 10^5
ZCT_1	12	-1.510	3.022	3618.00	23.120	4.320	-20.930
ZCT_2	18	-3.808	5.955	2752.00	27.520	3.633	-16.390
ZCT_3	24	-10.240	2.382	2116.00	29.630	3.375	-9.095
ZCT_4	30	-6.031	60.700	95.54	7.717	12.958	-2.035

4. Conclusion

Thin films of cobalt doped zinc oxide have been deposited on a microscopic glass substrates using chemical bath method. The deposited films were subjected to thickness, optical, structural, morphological and electrical characterizations to evaluate the effect of deposition time on these properties. Optical properties of the deposited films showed that absorbance values were high in the UV region and low in the VIS- region, while transmittance were high in the VIS region and low in the UV region. Owning to these characteristics, UV-radiations were screened off while visible and infra radiation were allowed or transmitted by the films. Energy band gap was estimated in the range of 3.38 eV and 3.41 eV. This confirmed the possibility of engineering of the cobalt doped zinc oxide by varying the deposition time as growth parameter. These findings from the optical properties of the deposited films make them potential material to be employed in solar thermal conversion and optoelectronic devices. The structural properties of the characterized film showed wurtzite structure typical of Zinc oxide material with grain sizes between the range of 14.90 nm and 21.50 nm. This result confirmed that the deposited films are nano films. Scanning electron micrograph of the characterized sample showed that the surface of the film composed of nanorods of slightly different sizes. Composition analysis of the film confirmed the presence of cobalt, zinc and oxygen.

Conflicts of Interest

The authors declare that there is no conflict of interest regarding the publication of this article.

Funding

This research received no specific grant from any funding agency in the public, commercial or not-for-profit sectors.

Reference

[1] Coleman, V.A.; Jagadish, C. Basic Properties and Applications of ZnO. *Processing, Properties and Applications,* 2006, 1-20, DOI: https://doi.org/10.1016/B978-008044722-3/50001-4.

[2] Cui J. Zinc oxide Nanowies, *Material Characterization,* 2012, 64, 43-52.

[3] Okoli, N.L.; Nkamuo, C.J.; Elekalachi, C.I. Effect of Dip Time on Electrodeposited Zinc Oxide Nanofilm. *American Journal of Materials Synthesis and Processing,* 2018, 3(2), 7-11.

[4] Oliveira F.F.; Proenca, M.P.; Araujo, J.P.; Ventura, J. Electrodeposition of ZnO thin films on conducting flexible substrates. *Journal of Materials Science,* 2016, 51(12), 5589-5597.

[5] Hassiba, R.; Rafiaa, K.; Abed, M.A.; Mokhtar, G.; Faycal, D. Electrodeposition and characterization of ZnO thin films using sodium thiosulfate as an additive for photovoltaic solar cells. *Journal of Semiconductors,* 2017, 38(5), 053002.

[6] Franklin, J.B.; Zou, B.; Petrov, P.; McComb, D.W.; Ryan, M.P.; McLachlan, M.A. Optimised pulsed laser deposition of ZnO thin films on transparent conducting substrates, *Journal of Materials Chemistry*, 2011, 21, 8178-8182.

[7] Ghafouri, V.; Shariati, M.; Ebrahimzad, A. Photoluminescence investigation of crystalline undoped ZnO nanostructures constructed by RF sputtering. *Scientia Iranica,* 2012, 19(3), 934-942.

[8] Norlida, K.; Muhd, F.K.; Roshida, R. Band Gap narrowing and widening of ZnO nanostructures and doped materials. *Nanoscale Research Letters,* 2015, 10, 346.

[9] Wallace, I.; Eshu, O.V.; Chukwunonso, O.B.; Okoro, U.C. Synthesis and Characterization of Zinc Oxide (ZnO) Nanowire. *Journal of Nanomedicine and Nanotechnology,* 2015, 6(5), 1000321.

[10] Ezenwa I.A. Synthesis and Optical Characterization of Zinc Oxide Thin Film, *Research Journal of Chemical Sciences,* 2012, 2(3), 26-30.

[11] Xianying, H.; Sebastian W.; Patritia, A.R.; Nicola. Cobalt Assisted Morphology and Assembly control of Co-Doped ZnO Nanoparticles. *Nano materials,* 2018, 8, 249.

[12] Rosmalini, A.K.; Nurmalina, M.T.; Wan, R.W.A.; Anees, A.A.; Ahmad, S.Z. Effect of substrates on Zinc Oxide thin films fabrication using sol-gel method. *IOP Conference Series: Materials Science and Engineering,* 2018, 340, 012002.

[13] Dhruvashi, K.R.; Shishodia, P.K. Growth of ZnO thin films doped with (Mn and Co) by spin coating technique. *American Insititute of physics,* 2016, 1728, 256.

[14] Febrianti, Y.; Putri, N.A.; Sugthartono, V.; Handoko, D. Synthesis and characterization of Co- doped zinc oxide nanorods prepared by Ultrasorric spray pyrolysis and hydrothermal method. *America Institute of Physics,* 2017, 1862, 030-056.

[15] Maciąg, A.; Sagan, P.; Kuźma, M.; Popovych, V. Zinc oxide films prepared by spray pyrolysis. *EPJ Web of Conferences,* 2017, 133, 03004.

[16] Karakaya, S.; Ozbaş, O. Deposition and Characterization of Zinc Oxide Films. *Journal of Natural and Applied Science,* 2013, 17(3), 49-51.

[17] Rongliang, H.; Bin, T.; Cuong, T.; Mathew, P. Physical structure and optical properties of Co-doped ZnO Nanoparticles prepared by Co-precipitation. *Journal of Nano particles Res.* 2013, 15, 2030.

[18] Ezema, F.I. Fabrication, optical properties and application of un-doped and application of un-doped chemical bath deposited ZnO thin films. *Journal of Research science,* 2004, 15, 343-350

[19] Okpala V.U.; Ezema I.F.; Osuji U.R. A Study of the Optical Properties of Un-doped and Potash doped Lead Chloride Crystal in Silica Gel. *Advances in Applied Sciences Research,* 2012, 3(1), 107.

[20] Dien, N.D. Preparation of various morphologies of ZnO nanostructure through wet chemical methods. *Advanced Materials Science,* 2019, 4, 1-5.

[21] Mohar, R.S.; Iwan, S.; Djuhana, D.; Imawan, C.; Harmoko, A.; Fauzia, V. Post-annealing effect on optical absorbance of hydrothermally grown zinc oxidenanorods. *AIP Conference Proceedings,* 2016, 1729(1), 020024.

[22] Rana, S.B.; Singh, P.; Sharma, A.K.; Carboonari, A.W.; Gogra R. Synthesis and characterization of pure and doped ZnO nanoparticles. *Journal of optoelectronics and Advanced materials,* 2010, 12(2), 257-261.

[23] Tay, M.C.; Pushpanathan, K.; Loanathan, M. Structural and Optical Properties of Co-doped ZnO Nanoparticles Synthesized by Precipitation Method. *Materials and Manufacturing Process,* 2014, 29, 771-779.

[24] Ueda, K.; Tabata, H.; Tamoji, K. Manetic and electric properties of transitional metal doped ZnO films. *Applied Physics letters*, 2001, 79(7), 988.